Competition between spin density wave order and superconductivity in the underdoped cuprates

Eun Gook Moon and Subir Sachdev
Department of Physics, Harvard University, Cambridge, Massachusetts 02138, USA
(Received 20 May 2009; revised manuscript received 17 June 2009; published 16 July 2009)

We describe the interplay between *d*-wave superconductivity and spin density wave (SDW) order in a theory of the hole-doped cuprates at hole densities below optimal doping. The theory assumes local SDW order, and associated electron and hole pocket Fermi surfaces of charge carriers in the normal state. We describe quantum and thermal fluctuations in the orientation of the local SDW order, which lead to *d*-wave superconductivity: we compute the superconducting critical temperature and magnetic field in a "minimal" universal theory. We also describe the back action of the superconductivity on the SDW order, showing that SDW order is more stable in the metal. Our results capture key aspects of the phase diagram of Demler *et al.* [Phys. Rev. Lett. **87**, 067202 (2001)] obtained in a phenomenological quantum theory of competing orders. Finally, we propose a finite temperature crossover phase diagram for the cuprates. In the metallic state, these are controlled by a "hidden" quantum critical point near optimal doping involving the onset of SDW order in a metal. However, the onset of superconductivity results in a decrease in stability of the SDW order, and consequently the actual SDW quantum critical point appears at a significantly lower doping. All our analysis is placed in the context of recent experimental results.

DOI: 10.1103/PhysRevB.80.035117 PACS number(s): 71.10.Hf, 75.10.Jm, 74.25.Dw

I. INTRODUCTION

A number of recent experimental observations have the potential to dramatically advance our understanding of the enigmatic underdoped regime of the cuprates. In the present paper, we will focus in particular on two classes of experiments (although our results will also have implications for a number of other experiments):

(i) The observation of quantum oscillations in the underdoped region of $YBa_2Cu_3O_{7-\delta}$ (YBCO).[1–6] The period of the oscillations implies a carrier density of order of the density of dopants. LeBoeuf *et al.*[6] have claimed that the oscillations are actually due to electronlike carriers of charge $-e$. We will accept this claim here, and show following earlier work,[7,8] in which it helps resolve a number of other theoretical puzzles in the underdoped regime.

(ii) Application of a magnetic field to the superconductor induces a quantum phase transition at a nonzero critical field, $H_{\rm sdw}$, involving the onset of spin density wave (SDW) order. This transition was first observed in $La_{2-x}Sr_xCuO_4$ with $x=0.144$ by Khaykovich *et al.*[9] Chang *et al.*[10,11] have provided detailed studies of the spin dynamics in the vicinity of $H_{\rm sdw}$, including observation of a gapped spin collective mode for $H<H_{\rm sdw}$ whose gap vanishes as $H\nearrow H_{\rm sdw}$. Most recently, such observations have been extended to $YBa_2Cu_3O_{6.45}$ by Haug *et al.*,[12] who obtained evidence for the onset of SDW order at $H\approx 15$ T. These observations were all on systems that do not have SDW order at $H=0$; they build on the earlier work of Lake *et al.*[13] who observed enhancement of preexisting SDW order at $H=0$ by an applied field in $La_{2-x}Sr_xCuO_4$ with $x=0.10$.

We begin our discussion of these experiments using the phenomenological quantum theory of the competition between superconductivity (SC) and SDW order.[14–17] The phase diagram in the work of Demler *et al.*[14] is reproduced in Fig. 1. The parameter t appears in a Landau theory of SDW order and tunes the propensity to SDW order, with SDW order being favored with decreasing t. We highlight a number of notable features of this phase diagram:

(A) The upper-critical field above which superconductivity is lost, H_{c2}, decreases with decreasing t. This is consistent with the picture of competing orders, as decreasing t enhances the SDW order, which in turn weakens the superconductivity.

(B) The SDW order is more stable in the nonsuperconducting "normal" state than in the superconductor. In other words, the line CM, indicating the onset of SDW order in the normal state, is to the right of point A where SDW order appears in the superconductor at zero field; i.e., $t_c(0)>t_c$. Thus inducing superconductivity destabilizes the SDW order, again as expected in a model of competing orders.

(C) An immediate consequence of feature B is the existence of the line AM of quantum phase transitions within the superconductor, representing $H_{\rm sdw}$, where SDW order appears with increasing H. As we have discussed above, this prediction of Demler *et al.*[14] has been verified in a number of experiments.

A related prediction by Demler *et al.*[14] that an applied current should enhance the SDW order also appears to have been observed in a recent muon spin-relaxation experiment.[18]

A glance at Fig. 1 shows that it is natural to place[19] the quantum oscillation experiments[1–6] in the nonsuperconducting phase labeled "SDW." Feature B above is crucial in this identification: the normal state reached by suppressing superconductivity with a field is a regime where SDW order is more stable. The structure of the Fermi surface in this normal state can be deduced in the framework of conventional spin density wave theory, and we recall the early results of Refs. 20 and 21 in Fig. 2. Recent studies[22,23] have extended these results to incommensurate ordering wave vectors **Q**, and find that the electron pockets (needed to explain the quantum oscillation experiments) remain robust under deviations from the commensurate ordering at (π,π). The present paper will consider only the case of commensurate ordering with **Q**

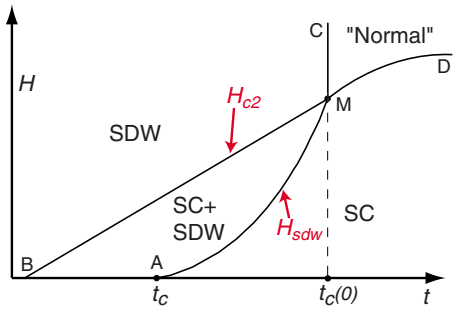

FIG. 1. (Color online) From Ref. 14: phase diagram of the competition between superconductivity (SC) and spin density wave (SDW) order tuned by an applied magnetic field H, and a Landau parameter t controlling the SDW order (the effective action has a term $t\vec{\varphi}^2$, where $\vec{\varphi}$ is the SDW order). The labels identifying H_{c2}, $H_{\rm sdw}$, and $t_c(0)$ have been added to the original figure (Ref. 14) but the figure is otherwise unchanged. The dashed line does not indicate any transition or crossover; it is just the continuation of the line CM to identify $t_c(0)$. A key feature of this phase diagram is that SDW order is more stable in the metal than in the superconductor, i.e., $t_c(0) > t_c$.

$=(\pi,\pi)$, as this avoids considerable additional complexity.

The above phenomenological theory appears to provide a satisfactory framework for interpreting the experiments highlighted in this paper. However, such a theory cannot ultimately be correct. A sign of this is that within its parameter space is a nonsuperconducting non-SDW normal state at $H=0$ and $T=0$ (not shown in Fig. 1). Indeed, such a state is the point of departure for describing the onset of the superconducting and SDW order in Ref. 14. There is no such physically plausible state, and the parameters were chosen so that this state does not appear in Fig. 1. Furthermore, we would like to extend the theory to spectral properties of the electronic excitations probed in numerous other experiments. This requires a more microscopic formulation of the theory of competing orders in terms of the underlying electrons. We shall provide such a theory here, building upon the proposals of Refs. 7, 8, 24, and 25. Our theory will not have the problematic $H=0$, $T=0$ normal state of the phenomenological theory, and so cannot be mapped precisely onto it. Nevertheless, we will see that our theory does reproduce the key aspects of Fig. 1. We will also use our theory to propose a finite temperature phase diagram for the hole-doped cuprates; in particular, we will argue that it helps resolve a central puzzle on the location of the quantum critical (QC) point important for the finite temperature crossovers into the "strange metal" phase. These results appear in Sec. IV and Fig. 10.

The theory of superconductivity,[27] mediated by exchange in quanta of the SDW order parameter $\vec{\varphi}$, has been successful above optimal doping. However, it does not appear to be compatible with the physics of competing orders in the underdoped regime, at least in its simplest version. This theory begins with the "large Fermi-surface" state in panel (d) of Fig. 2, and examines its instability in a BCS/Eliashberg theory due to attraction mediated by exchange in $\vec{\varphi}$ quanta. An increase in the fluctuations of $\vec{\varphi}$ is therefore connected to an increase in the effective attraction, and consequently a

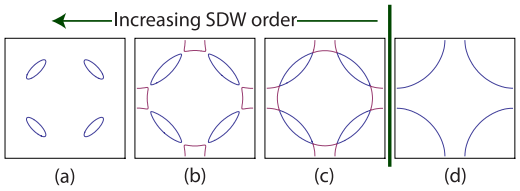

FIG. 2. (Color online) Fermi-surface evolution in the SDW theory (Refs. 20 and 21). Panel (d) is the large Fermi-surface state appropriate for the overdoped superconductor. The SDW order parameter, $\vec{\varphi}$, describes ordering at the wave vector $\mathbf{Q}=(\pi,\pi)$, and mixes fermion states whose wave vectors differ by $\mathbf{Q}$. This leads to the SDW metal state with electron (red) and hole (blue) pockets in panel (b), which is the state used here to explain the quantum oscillation experiments (Refs. 1–6).

strengthening of the superconducting order. This is evident from the increase in the critical temperature for superconductivity as the SDW ordering transition is approached from the overdoped side (see, e.g., Fig. 4 in Ref. 28). Thus rather than a competition, this theory yields an effective attraction between the SDW and superconducting order parameters. This was also demonstrated in Ref. 14 by a microscopic computation in this framework of the coupling between these order parameters. It is possible that these difficulties may be circumvented in more complex strong-coupling versions of this theory[28] but a simple physical picture of these is lacking.

As was already discussed in Ref. 14, the missing ingredient in the SDW theory of the ordering of the metal is the knowledge of the proximity to the Mott insulator in the underdoped compounds. Numerical studies of models in which the strong local repulsion associated with Mott insulator is implemented in a mean-field manner do appear to restore aspects of the picture of competing orders.[29,30] Here, we shall provide a detailed study of the model of the underdoped cuprates proposed in Refs. 7, 8, 24, and 25, and show that it is consistent with the features A–C of the theory of competing orders noted above, which are essential in the interpretation of the experiments.

As discussed at some length in Ref. 8, the driving force of the superconductivity in the underdoped regime is argued to be the pairing of the electron pockets visible in panel (b) of Fig. 2. Experimental evidence for this proposal also appeared in the recent photoemission experiments of Yang *et al.*[31] In the interests of simplicity, this paper will focus exclusively on the electron pockets, and neglect the effects of the hole pockets in Fig. 2. Further discussion on the hole pockets and the reason for their secondary role in superconductivity may be found in Refs. 8, 24, and 25.

The degrees of freedom of the theory are the bosonic spinons z_α ($\alpha=\uparrow,\downarrow$), and spinless fermions $g_\pm$. The spinons determine the local orientation of the SDW order via

$$\vec{\varphi} = z_\alpha^* \vec{\sigma}_{\alpha\beta} z_\beta, \tag{1.1}$$

where $\vec{\sigma}$ are the Pauli matrices. The electrons are assumed to form electron and hole pockets as indicated in Fig. 2(b) but with their components determined in a "rotating reference frame" set by the local orientation of $\vec{\varphi}$. This idea of Fermi surfaces correlated with the local order is supported by the

recent scanning tunnel microscopy (STM) observations of Wise *et al.*[32] Focusing only on the electron pocket components, we can write the physical electron operators c_α as[7,8]

$$c_\uparrow = e^{i\mathbf{G}_1\cdot\mathbf{r}}[z_\uparrow g_+ - z_\downarrow^* g_-] + e^{i\mathbf{G}_2\cdot\mathbf{r}}[z_\uparrow g_+ + z_\downarrow^* g_-],$$

$$c_\downarrow = e^{i\mathbf{G}_1\cdot\mathbf{r}}[z_\downarrow g_+ + z_\uparrow^* g_-] + e^{i\mathbf{G}_2\cdot\mathbf{r}}[z_\downarrow g_+ - z_\uparrow^* g_-], \quad (1.2)$$

where $\mathbf{G}_1=(0,\pi)$ and $\mathbf{G}_2=(\pi,0)$ are the antinodal points about which the electron pockets are centered. We present an alternative derivation of this fundamental relation from spin density wave theory in the Appendix.

Note that when $z_\alpha=(1,0)$, Eq. (1.1) shows that the SDW order is uniformly polarized in the z direction with $\vec{\varphi}=(0,0,1)$, and from Eq. (1.2) we have $c_\uparrow=g_+(e^{i\mathbf{G}_1\cdot\mathbf{r}}+e^{i\mathbf{G}_2\cdot\mathbf{r}})$ and $c_\downarrow=g_-(e^{i\mathbf{G}_1\cdot\mathbf{r}}-e^{i\mathbf{G}_2\cdot\mathbf{r}})$. Thus, for this SDW state, the $\pm$ labels on the $g_\pm$ are equivalent to the z spin projection, and the spatial dependence is the consequence of the potential created by the SDW order, which has opposite signs for the two spin components (as shown in the Appendix). The expression in Eq. (1.2) for general $\vec{\varphi}$ is then obtained by performing a spacetime-dependent spin rotation, determined by z_α, on this reference state.

Another crucial feature of Eqs. (1.1) and (1.2) is that the physical observables $\vec{\varphi}$ and c_α are invariant under the following U(1) gauge transformation of the dynamical variables z_α and $g_\pm$:

$$z_\alpha \to e^{i\phi} z_\alpha; \quad g_+ \to e^{-i\phi} g_+; \quad g_- \to e^{i\phi} g_-. \quad (1.3)$$

Thus the $\pm$ label on the $g_\pm$ can also be interpreted as the charge under this gauge transformation. This gauge invariance implies that the low energy effective theory will also include an emergent U(1) gauge field A_μ.

We will carry out most of the computations in this paper using a "minimal model" for z_α and $g_\pm$ with the imaginary time (τ) Lagrangian[7,8]

$$\mathcal{L} = \mathcal{L}_z + \mathcal{L}_g, \quad (1.4)$$

where the fermion action is

$$\mathcal{L}_g = g_+^\dagger \left[(\partial_\tau - iA_\tau) - \frac{1}{2m^*}(\boldsymbol{\nabla} - i\mathbf{A})^2 - \mu \right] g_+ + g_-^\dagger \left[(\partial_\tau + iA_\tau) - \frac{1}{2m^*}(\boldsymbol{\nabla} + i\mathbf{A})^2 - \mu \right] g_-, \quad (1.5)$$

and the spinon action is

$$\mathcal{L}_z = \frac{1}{t}\left\{ \sum_{\alpha=1}^{N} \left[|(\partial_\tau - iA_\tau) z_\alpha|^2 + v^2 |(\boldsymbol{\nabla} - i\mathbf{A}) z_\alpha|^2 \right] + i\varrho \left(\sum_{\alpha=1}^{N} |z_\alpha|^2 - N \right) \right\}. \quad (1.6)$$

Here the emergent gauge field is $A_\mu=(A_\tau,\mathbf{A})$, and, for future convenience, we have generalized to a theory with N spin components (the physical case is $N=2$). The field ϱ imposes a fixed length constraint on the z_α, and accounts for the self-interactions between the spinons.

This effective theory omits numerous other couplings involving higher powers or gradients of the fields, which have been discussed in some detail in previous work.[7,8,24,25] It also omits the $1/r$ Coulomb repulsion between the $g_\pm$ fermions—this will be screened by the Fermi-surface excitations, and is expected to reduce the critical temperature as in the traditional strong-coupling theory of superconductivity. For simplicity, we will neglect such effects here, as they are not expected to modify our main conclusions on the theory of competing orders. Nonperturbative effects of Berry phases are expected to be important in the superconducting phase, and were discussed earlier;[7] they should not be important for the instabilities toward superconductivity discussed here.

As has been discussed earlier,[7,8] the theory in Eq. (1.4) has a superconducting ground state with a simple momentum-independent pairing of the $g_\pm$ fermions $\langle g_+ g_- \rangle \neq 0$. Combining this pairing amplitude with Eq. (1.2), it is then easy to see[7,8] that the physical c_α fermions have the needed d-wave pairing signature (see Appendix).

The primary purpose of this paper is to demonstrate that the simple field theory in Eq. (1.4) satisfies the constraints imposed by the framework of the picture of competing orders. In particular, we will show that it displays the features A–C listed above. Thus, we believe it offers an attractive and unified framework for understanding a large variety of experiments in the underdoped cuprates. We also note that the competing order interpretation of Eq. (1.4) only relies on the general gauge structure of theory, and not specifically on the interpretation of $g_\pm$ as electron pockets in the antinodal region; thus it could also apply in other physical contexts.

Initially, it might seem that the simplest route to understanding the phase diagram of our theory [Eq. (1.4)] is to use it to compute the effective coupling constants in the phenomenological theory of Ref. 14. However, such a literal mapping is not possible because, as we discussed earlier, the phenomenological theory does have additional unphysical phases. Rather, we will show that our theory does satisfy the key requirements of the experimentally relevant phase diagram in Fig. 1.

A notable feature of the theory in Eq. (1.4) is that it is characterized by only two dimensionless couplings. We assume the chemical potential μ is adjusted to obtain the required fermion density, which we determine by the value of the Fermi wave vector k_F. The effective fermion mass m^* and the spin-wave velocity then determine our first dimensionless ratio

$$\alpha_1 \equiv \frac{\hbar k_F}{m^* v}. \quad (1.7)$$

Although we have inserted an explicit factor of $\hbar$ above, we will set $\hbar=k_B=1$ in most of our analysis. Note that we can also convert this ratio to that of the Fermi energy $E_F=\hbar^2 k_F^2/(2m^*)$ and the energy scale $m^* v^2$:

$$\frac{E_F}{m^* v^2} = \frac{\alpha_1^2}{2}. \quad (1.8)$$

From the values quoted in the quantum oscillation experiment,[1] $m^*=1.9m_e$ and $\pi k_F^2=5.1$ nm^{-2}, and the spin-wave velocity in the insulator $v\approx 670$ meV Å, we obtain the estimate $\alpha_1 \approx 0.76$. We will also use

$$m^* v^2 \approx 112 \text{ meV}, \tag{1.9}$$

as a reference energy scale.

The second dimensionless coupling controls the strength of the fluctuations of the SDW order, which are controlled by the parameter t in Eq. (1.6). Tuning this coupling leads to a transition from a phase with $\langle z_\alpha \rangle \neq 0$ to one where the spin rotation symmetry is preserved. We assume that this transition occurs at the value $t=t_c(0)$ in the metallic phase (the significance of the argument of t_c will become clear below): this corresponds to the line CM in Fig. 1. Then we can characterize the deviation from this quantum phase transition by the coupling

$$\alpha_2 \equiv \left(\frac{1}{t_c(0)} - \frac{1}{t} \right) \frac{1}{m^*}. \tag{1.10}$$

Note that $\alpha_2 < 0$ corresponds to the SDW phase in Fig. 1 while $\alpha_2 > 0$ corresponds to the normal phase of Fig. 1. For $\alpha_2 > 0$, we can also characterize this coupling by the value of the spinon energy gap Δ_z in the $N=\infty$ theory, which is (as will become clear below)

$$\frac{\Delta_z}{m^* v^2} = 4\pi\alpha_2. \tag{1.11}$$

It is worth noting here that our minimal model [Eq. (1.4)] in two spatial dimensions has aspects of the universal physics of the Fermi gas at unitarity in three spatial dimensions. The latter model has a "detuning" parameter that tunes the system away from the Feshbach resonance; this is the analog of our parameter α_2. The overall energy scale is set in the unitary Fermi gas by the Fermi energy; here, instead, we have two energy scales, E_F and $m^* v^2$.

The outline of the remainder of the paper is as follows. In Sec. II, we will consider the pairing problem of the $g_\pm$ fermions, induced by exchange in the gauge boson A_μ. We will do this within a conventional Eliashberg framework. Our main result will be a computation of the critical field H_{c2}, which will be shown to be suppressed as SDW order is enhanced with decreasing t. Section III will consider the feedback of the superconductivity on the SDW ordering, where we will find enhanced stability of the SDW order in the metal over the superconductor. Section IV will summarize our results, and propose a crossover phase diagram at nonzero temperatures.

II. ELIASHBERG THEORY OF PAIRING

In our minimal model, the charge and spin excitations interact with each other through the A_μ gauge boson. So the gauge fluctuation is one of the key ingredients in our analysis. We begin by computing the gauge propagator, and then we will determine the critical temperature and magnetic field within the Eliashberg theory in the following subsections.

We use the framework of the large N expansion. In the limit $N=\infty$, the gauge field is suppressed, and the constraint field ϱ takes a saddle-point value ($i\varrho = m^2$) that makes the spinon action extremum in Eq. (1.6). At leading order, the spinon propagator has the form

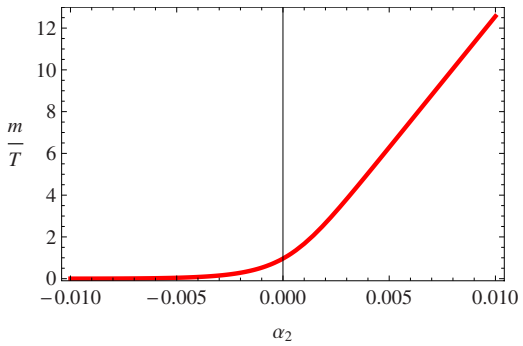

FIG. 3. (Color online) The parameter m in Eq. (2.1) for $T/(m^* v^2)=0.01$.

$$\frac{t}{v^2 k^2 + \omega_n^2 + m^2}, \tag{2.1}$$

where k is spatial momentum and ω_n is the Matsubara frequency. The saddle-point equation for m is

$$T \sum_{\omega_n} \int \frac{d^2k}{4\pi^2} \left[\frac{1}{v^2 k^2 + \omega_n^2 + m^2} \right] = -m^* \alpha_2 + \int \frac{d\omega}{2\pi} \int \frac{d^2k}{4\pi^2} \frac{1}{v^2 k^2 + \omega^2}. \tag{2.2}$$

The solution of this is

$$m = 2T \ln \left[\frac{e^{+2\pi m^* v^2 \alpha_2 / T} + \sqrt{e^{+4\pi m^* v^2 \alpha_2 / T} + 4}}{2} \right], \tag{2.3}$$

which holds for $-\infty < \alpha_2 < \infty$. This result is plotted in Fig. 3. Clearly, m is a monotonically increasing function of α_2. Recall that the positive α_2 region has no SDW order, and m is large here. As we will see below, the value of m plays a significant role in the photon propagators.

The photon propagator is determined from the effective action obtained by integrating out the spinons and nonrelativistic fermions. Using gauge invariance, we can write down the effective action of the gauge field as follows:

$$S_A = \frac{NT}{2} \sum_{\epsilon_n} \int \frac{d^2k}{4\pi^2} \left[(k_i A_\tau - \epsilon_n A_i)^2 \frac{D_1(k, \epsilon_n)}{k^2} + A_i A_j \left(\delta_{ij} - \frac{k_i k_j}{k^2} \right) D_2(k, \epsilon_n) \right]. \tag{2.4}$$

As in analogous computation with relativistic fermions in Ref. 33, we separate the photon polarizations into their bosonic and fermionic components:

$$D_1 = N D_{1b} + D_{1f},$$

$$D_2 = N D_{2b} + D_{2f}. \tag{2.5}$$

We use the Coulomb gauge $\mathbf{k} \cdot \mathbf{A} = 0$ in the computation. After imposing the gauge condition, the propagator of A_τ from the above action is $1/D_1$ while that of A_i is

$$\left(\delta_{ij}-\frac{k_ik_j}{k^2}\right)\frac{1}{D_2+(\epsilon_n^2/k^2)D_1}. \tag{2.6}$$

We will approximate D_{1b} and D_{2b} by their zero-frequency limits. Computation of the spinon polarization in this limit, as in Ref. 33, yields

$$D_{1b}(k)=-\frac{T}{\pi v^2}\ln\left[2\sinh\left(\frac{m}{2T}\right)\right]+\frac{1}{2\pi v^2}\int_0^1 dx\sqrt{m^2+v^2k^2x(1-x)}\times\coth\left(\frac{\sqrt{m^2+v^2k^2x(1-x)}}{2T}\right), \tag{2.7}$$

and

$$D_{2b}(k)=\frac{v^2k^2}{8\pi}\int_0^1 dx\frac{1}{\sqrt{m^2+v^2k^2x(1-x)}}\times\coth\left(\frac{\sqrt{m^2+v^2k^2x(1-x)}}{2T}\right). \tag{2.8}$$

For the fermionic contributions, we include the contribution of the $g_\pm$ fermions with effective mass m^* and Fermi wave vector k_F. Calculation of the fermion compressibility yields

$$D_{1f}(k,\epsilon_n)=2\int\frac{d^2q}{4\pi^2}\frac{[n_F(\varepsilon_{\mathbf{q}-\mathbf{k}/2})-n_F(\varepsilon_{\mathbf{q}+\mathbf{k}/2})]}{(i\epsilon_n+\mathbf{k}\cdot\mathbf{q}/m^*)}\approx\frac{m^*}{\pi}, \tag{2.9}$$

where n_F is the Fermi function. For the transverse propagator, we obtain from the computation of the fermion current correlations

$$\begin{aligned}D_{2f}(k,\epsilon_n)+\frac{\epsilon_n^2}{k^2}D_{1f}(k,\epsilon_n)&=\frac{k_F^2}{2\pi m^*}-\frac{2}{m^{*2}}\int\frac{d^2q}{4\pi^2}\times\left(q^2-\frac{(\mathbf{q}\cdot\mathbf{k})^2}{k^2}\right)\frac{[n_F(\varepsilon_{\mathbf{q}-\mathbf{k}/2})-n_F(\varepsilon_{\mathbf{q}+\mathbf{k}/2})]}{(i\epsilon_n+\mathbf{k}\cdot\mathbf{q}/m^*)}\\&\approx\frac{k_F|\epsilon_n|}{\pi k}.\end{aligned} \tag{2.10}$$

Putting all this together, we have the final form of the propagators. The propagator of A_τ is

$$\frac{1}{ND_{1b}(k)+m^*/\pi}, \tag{2.11}$$

while that of A_i is

$$\left(\delta_{ij}-\frac{k_ik_j}{k^2}\right)\frac{1}{ND_{2b}(k)+k_F|\epsilon_n|/(\pi k)}. \tag{2.12}$$

A. Eliashberg equations

We now address the pairing instability of the $g_\pm$ fermions. Both the longitudinal and transverse photons contribute an attractive interaction between the oppositely charged fermions, which prefers a simple s-wave pairing. However, we also know that the transverse photons destroy the fermionic quasiparticles near the Fermi surface, and so have a depairing effect. The competition between these effects can be addressed in the usual Eliashberg framework.[34] Based upon arguments made in Refs. 35 and 36, we can anticipate that the depairing and pairing effects of the transverse photons exactly cancel each other in the low-frequency limits because of the s-wave pairing. The higher frequency photons yield a net pairing contribution below a critical temperature T_c, which we compute below.

Closely related computations have been carried out by Chubukov and Schmalian[37] on a generalized model of pairing due to the exchange in a gapless bosonic collective mode; our numerical results for T_c below agree well with theirs, where the two computations can be mapped onto each other.[38]

The Eliashberg approximation starts from writing the fermion Green function using Nambu spinor notation.

$$\hat{\Sigma}(\omega_n)=i\omega_n[1-Z(\omega_n)]\hat{\tau}_0+\epsilon\hat{\tau}_3+\phi(\omega_n)\hat{\tau}_1,$$

$$G^{-1}(\epsilon,\omega_n)=i\omega_nZ(\omega_n)\hat{\tau}_0-\epsilon\hat{\tau}_3-\phi(\omega_n)\hat{\tau}_1, \tag{2.13}$$

where $\hat{\tau}$ are the Pauli matrices in the particle-hole space. Then self-consistency equation is constructed by evaluating the self-energy with the above Green's function, which yields the following equation:

$$\begin{aligned}\hat{\Sigma}(\omega_n)&=T\sum_{\omega_m}\int\frac{d^2k'}{4\pi^2}\hat{G}(k',\omega_m)\tilde{D}(\vec{q},\vec{k},\omega_m-\omega_n)\\&=T\sum_{\omega_m}\lambda^{\mathrm{tot}}(\omega_m-\omega_n)\int d\epsilon'\hat{G}(\epsilon',\omega_m).\end{aligned} \tag{2.14}$$

Note that the first line is a formal expression, with $\tilde{D}(\vec{q},\vec{k},i\omega_m)$ being a combination of the photon propagator and the matrix elements of the vertex. The equations are therefore characterized by the coupling $\lambda^{\mathrm{tot}}(\omega_n)$; computation of the photon contribution yields the explicit expression[39,40]

$$\lambda^{\mathrm{tot}}(\omega_n)=\lambda_T(\omega_n)+\lambda_L,$$

$$\lambda_T(\omega_n)=\frac{k_F}{2\pi^2m^*}\int_0^{2k_F}dk\frac{\sqrt{1-(k/2k_F)^2}}{ND_{2b}(k)+k_F|\omega_n|/(\pi k)}, \tag{2.15}$$

$$\lambda_L=\frac{m^*}{2\pi^2k_F}\int_0^{2k_F}\frac{dk}{\sqrt{1-(k/2k_F)^2}}\left[\frac{1}{ND_{1b}(k)+m^*/\pi}\right]. \tag{2.16}$$

We have divided the total coupling into two pieces based on the different frequency dependence of the longitudinal and transversal gauge boson propagators. The frequency independent term will need a cutoff for the actual calculation as we will see below. The typical behaviors of the dimensionless couplings $\lambda_T(\omega_n),\lambda_L$ are shown in Fig. 4.

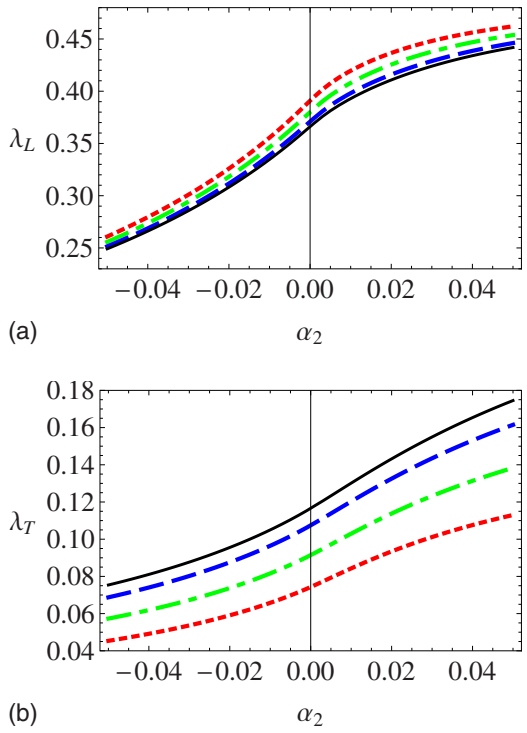

FIG. 4. (Color online) The pairing coupling constants associated with the longitudinal (λ_L) and transverse [$\lambda_T(\omega_n)$] gauge interactions. The parameter α_2 measures the distance from the SDW ordering transition in the metal, as defined in Eq. (1.10). The dotted (red), dot-dashed (green), dashed (blue), and continuous (black) lines correspond to $\alpha_1^2/2=E_F/(m^*v^2)=0.16,0.21,0.26,0.29$. We show $\lambda_T(\omega_n=8\pi T)$ with $T/(m^*v^2)=0.016$ for the transverse interaction. Note that $\lambda_T(\omega_n)$ function is analytic near $\alpha_2\sim 0$ in the magnified scale.

The longitudinal coupling λ_L is around 0.35, and has a significant dependence upon α_2, which is a measure of the distance from the SDW ordering transition. Note that λ_L is *larger* in the SDW-disordered phase ($\alpha_2>0$): this is a consequence of the enhancement of gauge fluctuations in this regime. This will be the key to the competing order effect we are looking for: gauge fluctuations, and hence superconductivity, is enhanced when the SDW order is suppressed.

The transverse gauge fluctuations yield the frequency-dependent coupling $\lambda_T(\omega_n)$. This is divergent at low frequencies with[39,40] $\lambda_T(\omega_n)\sim|\omega_n|^{-1/3}$. As we noted earlier, this divergent piece cancels out between the normal and anomalous contributions to the fermion self-energy.[35,36] We plot the dependence of $\lambda_T(\omega_n)$ on the coupling α_2 for a fixed ω_n in Fig. 4. As was for the case of the longitudinal coupling, the transverse contribution is larger in the SDW-disordered phase.

The full self-consistent Eliashberg equations are obtained by matching the coefficients of the Pauli matrices term by term.

$$i\omega_n[1-Z(\omega_n)]=-\pi T\sum_{\omega_m}\lambda^{\mathrm{tot}}(\omega_m-\omega_n)\frac{i\omega_m}{\sqrt{\omega_m^2+\Delta^2(\omega_m)}}, \tag{2.17}$$

$$Z(\omega_n)\Delta(\omega_n)=\pi T\sum_{\omega_m}\lambda^{\mathrm{tot}}(\omega_m-\omega_n)\frac{\Delta(\omega_m)}{\sqrt{\omega_m^2+\Delta^2(\omega_m)}}, \tag{2.18}$$

where $\Delta(\omega_n)$ is the frequency-dependent pairing amplitude.

Now we can solve the self-consistent equations to determine the boundary of the superconducting phase. Our goal is to look for the critical temperature and magnetic field, and we can linearize the equations in $\Delta(\omega_n)$ in these cases; in other words we would neglect the gap functions in the denominator.

$$Z(\omega_n)=1+\frac{\pi T}{\omega_n}\sum_{\epsilon_n}\mathrm{sgn}(\epsilon_n)\lambda_T(\omega_n-\epsilon_n)$$
$$=1+\frac{\pi T}{|\omega_n|}\sum_{|\epsilon_n|<|\omega_n|}\lambda_T(\epsilon_n). \tag{2.19}$$

Then the solution of the critical temperature of linearized Eliashberg equation is equivalent to the condition that the matrix $K(\omega_n,\omega_m)$ first has a positive eigenvalue, where

$$K(\omega_n,\omega_m)=\lambda_T(\omega_n-\omega_m)+\lambda_L\Lambda(\omega_n-\omega_m)-\delta_{n,m}\frac{|\omega_n|Z(\omega_n)}{\pi T}, \tag{2.20}$$

with the soft cutoff function with cutoff E_F

$$\Lambda(\omega_n)\equiv\frac{1}{1+c_1(\omega_n/E_F)^2}, \tag{2.21}$$

where c_1 is a constant of order unity. The cutoff E_F is the highest energy scale of the electronic structure so it is not unnatural to set the cutoff with the scale. With this, the numerics is well defined and we plot the resulting critical temperature in Fig. 5.

For comparison, we show in Fig. 6 the results for T_c obtained in a model with only the transverse interaction associated with $\lambda_T(\omega_n)$. We can use this T_c to define an effective transverse coupling, $\bar{\lambda}_T$, by $T_c/E_F=\exp(-1/\bar{\lambda}_T)$. Using $T_c/E_F\approx 0.008$ for $\alpha_2\approx 0$ in Fig. 6, we obtain $\bar{\lambda}_T\approx 0.2$. This is of the same order as the longitudinal coupling λ_L for $\alpha_2\approx 0$ in Fig. 4.

Bigger attractive interactions $\lambda_T(\omega_n)$ and λ_L clearly induce a higher critical temperature in the SDW-disordered region. Note that this behavior is different from the one of previous SDW-mediated superconductivity.[27] (See the results of Fig. 4 in Ref. 28; near the critical region, T_c shows the opposite behavior there.) We have also compared the plots obtained by scaling T_c by m^*v^2 and E_F. The dependencies on the parameter α_1 are reversed in two plots in the SDW-disordered region. To interpret α_1 as the doping related parameter, we should choose the scaling by m^*v^2 because the mass m^* and spin-wave velocity v are not affected much by doping. With this scaling (the first plot in Fig. 5), the critical temperature rises with increased doping at fixed α_2; of course, in reality, α_2 is also an increasing function of doping.

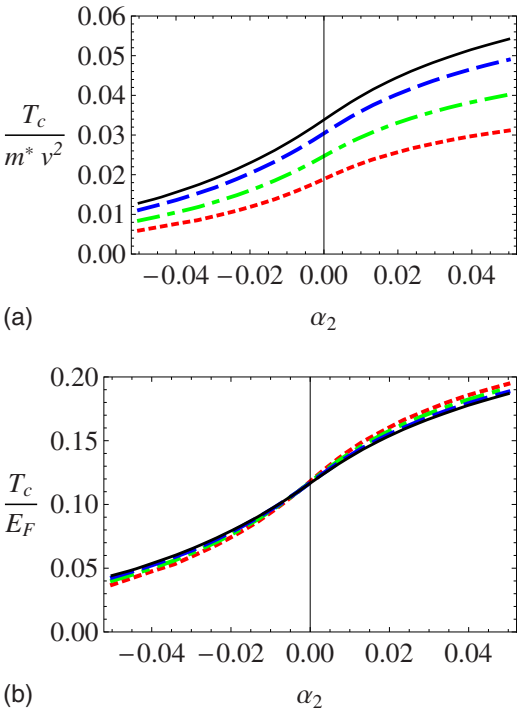

FIG. 5. (Color online) The critical temperature for superconductivity obtained by solution of the Eliashberg equations. The lines are for the same parameter values as in Fig. 4. The top plot has critical temperature scaled with $m^* v^2$, and the bottom is one scaled with E_F.

B. Critical field

This subsection will extend the above analysis to compute the upper-critical magnetic field, H_{c2} at $T=0$. We will neglect the weak Zeeman coupling of the applied field, and assume that it couples only to the orbital motion of the $g_\pm$ fermions. This means that $\mathcal{L}_g$ in Eq. (1.5) is modified to

$$\mathcal{L}_g = g_+^\dagger \left\{ (\partial_\tau - iA_\tau) - \frac{1}{2m^*}[\nabla - i\mathbf{A} - i(e/c)\mathbf{a}]^2 - \mu \right\} g_+ + g_-^\dagger \left\{ (\partial_\tau + iA_\tau) - \frac{1}{2m^*}[\nabla + i\mathbf{A} - i(e/c)\mathbf{a}]^2 - \mu \right\} g_-, \tag{2.22}$$

where $\nabla \times \boldsymbol{a} = H$ is the applied magnetic field.

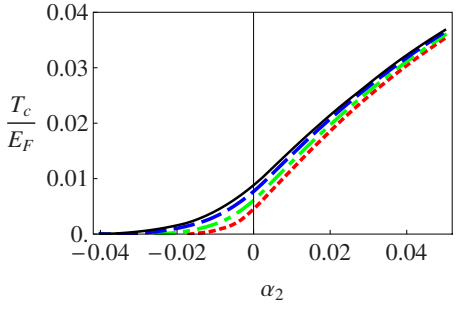

FIG. 6. (Color online) As in the top panel of Fig. 5 but with only the transverse pairing interaction, $\lambda_T(\omega_n)$, included.

Generally, the magnetic field induces nonlocal properties in the Green's function. However, in the vanishing gap limit, Helfand and Werthamer proved that the nonlocality only appears as a phase factor (see Ref. 41). The formalism has been developed by Shossmann and Schachinger,[42] and we will follow their method. As they showed, in the resulting equation for H_{c2}, the magnetic field only appears in the modification of the frequency renormalization $Z(\omega_n)$.

The Eliashberg equations in zero magnetic contain a term $|\omega_n Z(\omega_n)|$, which comes from the inverse of the cooperon propagator type at momentum $q=0$, $C(\omega_n,0)$, where

$$\begin{aligned} C(\omega_n,q) &= \int \frac{d^2p}{4\pi^2} \frac{1}{[-i\omega_n Z(\omega_n) + \varepsilon_{\mathbf{p}+\mathbf{q}}][i\omega_n Z(\omega_n) + \varepsilon_{-\mathbf{p}}]} \\ &\approx N(0) \int_0^{2\pi} \frac{d\theta}{2\pi} \int_{-\infty}^{\infty} d\varepsilon \\ &\quad \times \frac{1}{[-i\omega_n Z(\omega_n) + \varepsilon + v_F q \cos\theta][i\omega_n Z(\omega_n) + \varepsilon]} \\ &= \frac{2\pi N(0)}{\sqrt{4\omega_n^2 Z^2(\omega_n) + v_F^2 q^2}}, \end{aligned} \tag{2.23}$$

where $N(0)$ is the density of states at the Fermi level per spin.

Now we discuss the extension of this to $H=0$, as described in Refs. 41–43. For this, we need to replace $C(\omega_n,0)$ by the smallest eigenvalue of the operator

$$\hat{\mathcal{L}}(\omega_n) = \int d^2\rho \int \frac{d^2q}{4\pi^2} C(\omega_n,q) e^{i\mathbf{q}\cdot\boldsymbol{\rho}} e^{-i\boldsymbol{\rho}\cdot\hat{\boldsymbol{\pi}}}, \tag{2.24}$$

where $\hat{\boldsymbol{\pi}} = \hat{\mathbf{p}} - (2e/\hbar c)\mathbf{A}(\hat{\mathbf{r}})$. Using Eq. (22) from Ref. 43, we find that the smallest eigenvalue of $\hat{\mathcal{L}}(\omega_n)$ is

$$\begin{aligned} \mathcal{L}_0(\omega_n) &= \int_0^\infty \rho d\rho \int_0^\infty q dq J_0(q\rho) C(\omega_n,q) e^{-\rho^2/(2r_H^2)} \\ &= r_H^2 \int_0^\infty q dq e^{-q^2 r_H^2/2} C(\omega_n,q), \end{aligned} \tag{2.25}$$

where $r_H = \sqrt{\hbar c/2eH}$ is the magnetic length.

So the only change in the presence of a field is that the wave-function renormalization $Z(\omega_n)$ is replaced by $Z_H(\omega_n)$, where

$$\frac{1}{Z_H(\omega_n)} = 2|\omega_n| r_H^2 \int_0^\infty q dq \frac{e^{-q^2 r_H^2/2}}{\sqrt{4\omega_n^2 Z^2(\omega_n) + v_F^2 q^2}} \tag{2.26}$$

$$= 2|\omega_n| \int_0^\infty x dx \frac{e^{-x^2/2}}{\sqrt{4\omega_n^2 Z^2(\omega_n) + v_F^2 r_H^{-2} x^2}}. \tag{2.27}$$

We can now insert the modified $Z(\omega_n)$ in Eq. (2.27) into Eq. (2.20), and so compute H_{c2} as a function of both α_1 and the SDW tuning parameter α_2. The natural scale for the magnetic field is

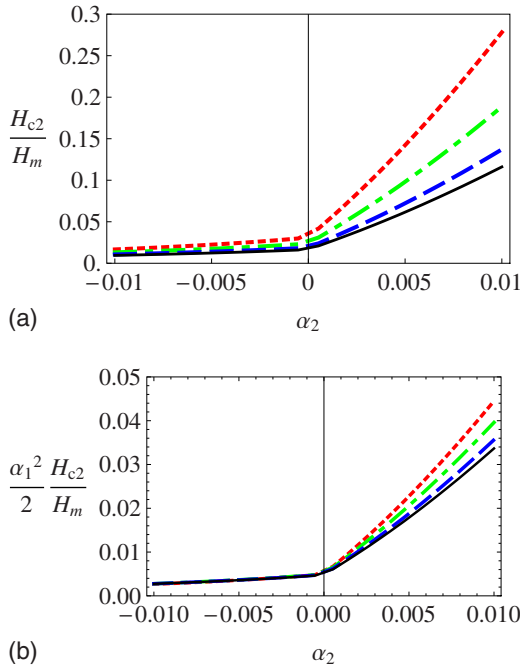

FIG. 7. (Color online) The upper-critical field H_{c2} as a function of α_1 and α_2 using the same conventions as in Fig. 4. The magnetic field is measured with the units induced by the fermion mass via H_m defined in Eq. (2.28).

$$H_m \equiv \left(\frac{\hbar c}{2e}\right) k_F^2 \approx 534 \text{ T}, \tag{2.28}$$

where in the last step we have used values from the quantum oscillation experiment[1] quoted in Sec. I. Our results for H_{c2}/H_m are shown in Fig. 7. We can see that the critical-field dependence on α_2 is similar to the critical temperature dependence: it is clear that SDW competes with superconductivity, and that H_{c2} decreases as the SDW ordering is enhanced by decreasing α_2. Also, we can compare this with the phenomenological phase diagram of Fig. 1; the critical-field line in Fig. 7 determines the line B-M-D within Eliashberg approximation. Finally, the values of H_{c2} in Fig. 7 are quite compatible with the quantum oscillation experiments.[1–6]

III. SHIFT OF SDW ORDERING BY SUPERCONDUCTIVITY

We are interested in the feedback on the strength of magnetic order due to the onset of superconductivity. Rather than using a self-consistent approach, we will address the question here systematically in a $1/N$ expansion.

We will replace the fermion action in Eq. (1.5) by a theory that has $N/2$ copies of the electron pockets

$$\mathcal{L}_g = \sum_{a=1}^{N/2} \left\{ g_{+a}^\dagger \left[(\partial_\tau - iA_\tau) - \frac{1}{2m^*}(\nabla - i\mathbf{A})^2 - \mu \right] g_{+a} + g_{-a}^\dagger \times \left[(\partial_\tau + iA_\tau) - \frac{1}{2m^*}(\nabla + i\mathbf{A})^2 - \mu \right] \times g_{-a} - \Delta g_{+a} g_{-a} - \Delta g_{-a}^\dagger g_{+a}^\dagger \right\}. \tag{3.1}$$

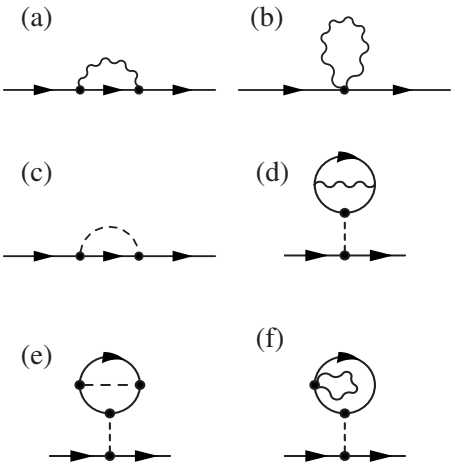

FIG. 8. Feynman diagrams for the self-energy of z_α from Ref. 33. The full line represents z_α, the wavy line is the A_μ propagator, and the dashed line is the ϱ propagator, which imposes the length constraint on z_α.

Here we consider the gauge boson fluctuation more rigorously in the sense of accounting for full fermion and boson polarization functions. But we will treat the fermion pairing amplitude Δ as externally given: the previous section described how it could be determined in the Eliashberg theory with approximated polarization.

The large N expansion proceeds by integrating out the z_α and the $g_{\pm a}$, and then expanding the effective action for ϱ and A_μ—formally this has the same structure as the computation in Ref. 33, generalized here to nonrelativistic fermions. At $N=\infty$, the $g_{\pm a}$ and z_α remain decoupled because the gauge propagator is suppressed by a prefactor of $1/N$. So at this level, the magnetic critical point is not affected by the presence of the fermions, and appears at $t=t_c^0$, where

$$\frac{1}{t_c^0} = \int \frac{d\omega d^2k}{8\pi^3} \frac{1}{\omega^2 + v^2k^2}. \tag{3.2}$$

We are interested in determining the $1/N$ correction to the magnetic quantum critical point, which we write as

$$\frac{1}{t_c(\Delta)} = \frac{1}{t_c^0} + \frac{1}{N}F(\Delta), \tag{3.3}$$

note that in the notation of Fig. 1, $t_c \equiv t_c(\Delta)$. The effect of superconductivity on the magnetic order will therefore be determined by $F(\Delta)-F(0)$, which is the quantity to be computed. The shift of the critical point at this order will be determined by the graphs in Fig. 3 of Ref. 33, which are reproduced here in Fig. 8. Evaluating these graphs we find

$$F(\Delta) = \int \frac{d^2q d\omega}{8\pi^3} \int \frac{d^2p d\epsilon}{8\pi^3} \frac{1}{(\epsilon^2 + v^2p^2)^2} \times \left[\frac{1}{D_1(q,\omega)} \left(\frac{(2\epsilon+\omega)^2}{(\epsilon+\omega)^2 + v^2(p+q)^2} - \frac{\omega^2}{\omega^2 + v^2q^2} \right) + \frac{1}{[D_2(q,\omega) + (\omega^2/q^2)D_1(q,\omega)]} \right.$$

$$\times\left(\frac{4v^4(p^2-(pq)^2/q^2)}{(\epsilon+\omega)^2+v^2(p+q)^2}\right)+\frac{1}{\Pi_\varrho(q,\omega)}$$
$$\times\left(\frac{1}{\omega^2+v^2q^2}-\frac{1}{(\omega+\epsilon)^2+v^2(p+q)^2}\right)\Bigg], \tag{3.4}$$

where $1/\Pi_\varrho(q,\omega)=8\sqrt{\omega^2+v^2q^2}$ is the propagator of the Lagrange multiplier field ϱ. The last term involving Π_ϱ is independent of Δ, and so will drop out of our final expressions measuring the influence of superconductivity: we will therefore omit this term in subsequent expressions for $F(\Delta)$.

It is now possible to evaluate the integrals over p and ϵ analytically. This is done by using a relativistic method in three space/time dimensions. Using a three-momentum notation in which $P_\mu\equiv(vp_i,\epsilon)$ and $Q_\mu\equiv(vq_i,\omega)$, and $\int_P \equiv v^2\int d\epsilon d^2p/(8\pi^3)$, some useful integrals obtained by dimensional regularization are

$$\int_P \frac{1}{P^4}=0,$$

$$\int_P \frac{1}{P^4(P+Q)^2}=0,$$

$$\int_P \frac{P_\mu}{P^4(P+Q)^2}=-\frac{Q_\mu}{16Q^3},$$

$$\int_P \frac{P_\mu P_\nu}{P^4(P+Q)^2}=\frac{\delta_{\mu\nu}}{32Q}+\frac{Q_\mu Q_\nu}{32Q^3}. \tag{3.5}$$

While some of the integrals above appear infrared divergent, there are no infrared divergencies in the complete original expression in Eq. (3.4), and we have verified that dimensional regularization does indeed lead to the correct answer obtained from a more explicit subtraction of the infrared singularities. Using these integrals, we obtain from Eq. (3.4)

$$F(\Delta)=\int\frac{d^2qd\omega}{8\pi^3}\frac{q^2}{8(\omega^2+v^2q^2)^{1/2}}\Bigg[\frac{1}{(\omega^2+v^2q^2)D_1(q,\omega)}$$
$$+\frac{1}{q^2D_2(q,\omega)+\omega^2D_1(q,\omega)}\Bigg]. \tag{3.6}$$

The above expression was obtained in the Coulomb gauge but we have verified that it is indeed gauge invariant.

We can now characterize the shift of the critical point in the superconductor by determining the spinon gap, Δ_z, at the coupling $t=t_c(0)$, where there is an onset of magnetic order in the metal, i.e., the spinon gap in the superconductor at $H=0$ at the value of t corresponding to the line CM in Fig. 1. To leading order in $1/N$, this is given by

$$\frac{\Delta_z}{m^*v^2}=\frac{4\pi}{m^*}\left[\frac{1}{t_c(\Delta)}-\frac{1}{t_c(0)}\right]=\frac{4\pi}{m^*N}[F(\Delta)-F(0)]. \tag{3.7}$$

This expression encapsulates our main result on the back action of the superconductivity of the $g_\pm$ fermions, with pairing gap Δ, on the position of the SDW ordering transition.

Before we can evaluate Eq. (3.7), we need the gauge-field propagators $D_{1,2}$. For completeness, we give explicit expressions for the boson and fermionic contributions by writing

$$D_2(q,\omega)+\frac{\omega^2}{q^2}D_1(q,\omega)=D_T^b(q,\omega)+D_T^f(q,\omega), \tag{3.8}$$

$$D_1(q,\omega)=D_L^b(q,\omega)+D_L^f(q,\omega). \tag{3.9}$$

We can read off the bosonic polarization functions $D_{L,T}^b(q,\omega)$ from the exact relativistic result of Ref. 33, and Eq. (2.4).

$$D_T^b(q,\omega)=\frac{\sqrt{v^2q^2+\omega^2}}{16}, \tag{3.10}$$

$$D_L^b(q,\omega)=\frac{1}{16}\frac{q^2}{\sqrt{v^2q^2+\omega^2}}. \tag{3.11}$$

For the fermion contribution, let us introduce the Nambu spinor Green's function

$$\bar g(q,\omega)=\frac{1}{(i\omega)^2-E_q^2}\begin{pmatrix} i\omega+\xi_q & -\Delta \\ -\Delta & i\omega-\xi_q\end{pmatrix} \tag{3.12}$$

$$=\int\frac{d\Omega}{\pi}\frac{1}{\Omega-i\omega}\mathrm{Im}[\bar g(q,\Omega)], \tag{3.13}$$

$$\mathrm{Im}[\bar g(q,\Omega)]=\frac{(-\pi)}{2E_q}(\delta(\Omega-E_q)-\delta(\Omega+E_q))$$
$$\times\begin{pmatrix}\Omega+\xi_q & -\Delta\\ -\Delta & \Omega-\xi_q\end{pmatrix}, \tag{3.14}$$

where $\xi_q=q^2/(2m^*)-\mu$ and $E_q=\sqrt{\xi_q^2+\Delta^2}$. With the matrix elements of longitudinal and transverse parts, the polarizations of the fermions are

$$D_L^f(q,\omega)=-\int\frac{d^2k}{(2\pi)^2}\frac{d\epsilon}{(2\pi)}\mathrm{tr}[\bar g(k,\epsilon)\bar g(q+k,\omega+\epsilon)]$$
$$=\int\frac{d^2k}{(2\pi)^2}\int\frac{d\Omega'}{\pi}\frac{d\Omega}{\pi}\frac{n_F(\Omega')-n_F(\Omega)}{i\omega+\Omega-\Omega'}$$
$$\times\mathrm{tr}[\mathrm{Im}\,\bar g(k,\Omega)\mathrm{Im}\,\bar g(q+k,\Omega')]$$
$$=\int\frac{d^2k}{(2\pi)^2}\frac{1}{2}\left(1-\frac{\xi_k\xi_{k+q}+\Delta^2}{E_kE_{k+q}}\right)\left(\frac{2(E_k+E_{k+q})}{\omega^2+(E_k+E_{k+q})^2}\right),$$

$$D_T^f(q,\omega)=D_{T,\mathrm{dia}}^f+D_{T,\mathrm{para}}^f, \tag{3.15}$$

$$D_{T,\mathrm{para}}^f=-\int\frac{d^2k}{(2\pi)^2}\frac{1}{(m^*)^2}\left(k^2-\frac{(kq)^2}{q^2}\right)\int\frac{d\epsilon}{(2\pi)}$$
$$\times\mathrm{tr}[\bar g(k,\epsilon)\hat\tau_3\bar g(q+k,\omega+\epsilon)\hat\tau_3]$$
$$=-\int\frac{d^2k}{(2\pi)^2}\frac{k^2\sin^2\theta}{(m^*)^2}\int\frac{d\Omega}{\pi}\frac{d\Omega'}{\pi}\frac{n_F(\Omega')-n_F(\Omega)}{i\omega+\Omega-\Omega'}$$
$$\times\mathrm{tr}[\mathrm{Im}\,\bar g(k,\Omega)\hat\tau_3\,\mathrm{Im}\,\bar g(q+k,\Omega')\hat\tau_3]$$
$$=-\int\frac{d^2k}{(2\pi)^2}\frac{k^2\sin^2\theta}{(m^*)^2}\frac{1}{2}\left(1-\frac{\xi_k\xi_{k+q}-\Delta^2}{E_kE_{k+q}}\right)$$

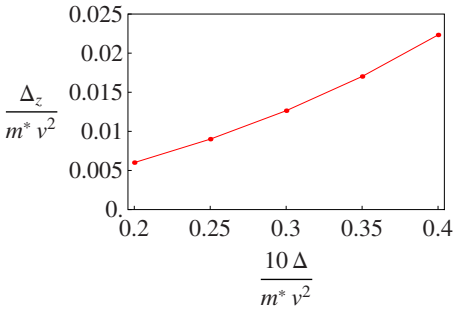

FIG. 9. (Color online) The energy Δ_z in Eq. (3.7) determining the value of the shift in the SDW ordering critical point, $t_c(0) - t_c(\Delta)$. The horizontal axis is the externally given superconducting gap. For numerics we fix the parameter $\alpha_1/2 = E_F/m^* v^2 = 0.3$

$$\times \frac{2(E_k + E_{k+q})}{\omega^2 + (E_k + E_{k+q})^2}\Bigg), \tag{3.16}$$

$$D^f_{T,\mathrm{dia}} = \frac{\rho_f}{m^*}, \tag{3.17}$$

where ρ_f is the density of the fermions and $\hat{\tau}_3$ is a Pauli matrix in the Nambu particle-hole space. With these results we are now ready to evaluate Eq. (3.7).

One of the key features of the theory of competing orders was the enhanced stability of SDW ordering in the metallic phase. This corresponds to feature B discussed in Sec. I: $t_c(0) > t_c$ in Fig. 1. In the notation of our key result in Eq. (3.7), where $t_c(\Delta) \equiv t_c$, this requires $\Delta_z > 0$. We show numerical evaluations of Eq. (3.7) in Fig. 9 and find this indeed is the case. (The values of Δ used in Fig. 9 are similar to those obtained in Sec. II near the SDW ordering critical point.) Indeed, the sign of Δ_z is easily understood. In the metallic phase, the gauge fluctuations are quenched by excitations of the Fermi surface. On the other hand, in the superconducting state, this effect is no longer present: gauge fluctuations are enhanced and hence SDW ordering is suppressed. Note the fact that the $g_\pm$ fermions having opposite gauge charges is crucial to this conclusion. The ordinary Coulomb interaction, under which the $g_\pm$ have the same charge, continues to be screened in the superconductor. In contrast, a gauge force that couples with opposite charges has its polarizability strongly suppressed in the superconductor, much like the response of a BCS superconductor to a Zeeman field.

IV. CONCLUSIONS

This paper has described the phase diagram of a simple minimal model of the underdoped hole-doped cuprates contained in Eqs. (1.4)–(1.6). This theory describes bosonic neutral spinons z_α and spinless charge $-e$ fermion $g_\pm$ coupled via a U(1) gauge field A_μ. We have shown that the theory reproduces key aspects of a phenomenological phase diagram[14,16] of the competition between SDW order and superconductivity in Fig. 1 in an applied magnetic field, H. This phase diagram has successfully predicted a number of recent experiments, as was discussed in Sec. I.

In particular, in Sec. II, we showed that the minimal model had a H_{c2} that decreased as the SDW ordering was enhanced by decreasing the coupling t in Eq. (1.6).

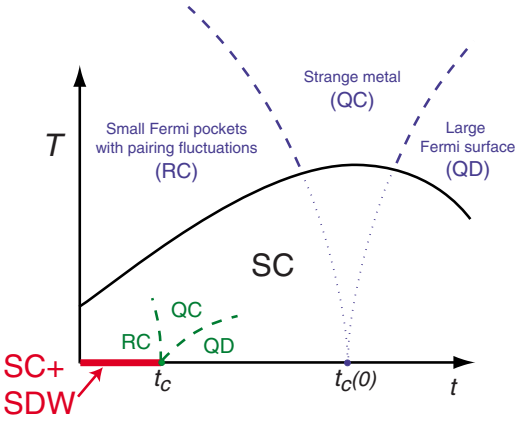

FIG. 10. (Color online) Proposed finite temperature crossover phase diagram for the cuprates. The labels at $T=0$ are as in Fig. 1: the onset of SDW order in the superconductor is at $t_c \equiv t_c(\Delta)$, while $t_c(0)$ is a "hidden" critical point that can be observed only at $H > H_{c2}$ as in Fig. 1. The computations in Sec. III show that $t_c(0) > t_c(\Delta)$. The full line is the phase transition at T_c representing loss of superconductivity. The dashed lines are crossovers in the fluctuations of the SDW order. The dotted lines are guides to the eye and do not represent any crossovers. Thus, in the pseudogap regime at $T > T_c$ the SDW fluctuations are in the RC (Ref. 26) regime; upon lowering temperature, they crossover to the QC and QD regimes in the superconductor.

Next, in Sec. III, we showed that the onset of SDW ordering in the normal state with $H > H_{c2}$ occurred at a value $t = t_c(0)$, which was distinct from the value $t = t_c(\Delta)$ in the superconducting state with $H=0$. As expected from the competing order picture in Fig. 1, we found $t_c(0) > t_c(\Delta)$. The enhanced stability of SDW ordering in the metal was a consequence of the suppression of A_μ gauge fluctuations by the $g_\pm$ Fermi surfaces. These Fermi surfaces are absent in the superconductor, and as a result the gauge fluctuations are stronger in the superconductor.

We conclude this paper by discussing the implications of our results for the phase diagram at $T > 0$, and in particular for the pseudogap regime above T_c. In our application of the main result in Sec. III, $t_c(0) > t_c(\Delta)$, we have assumed that the $\Delta = 0$ state was reached by application of a magnetic field. However, this result also applies if Δ is suppressed by thermal fluctuations above T_c. Unlike H, thermal fluctuations will also directly affect the SDW order, in addition to the indirect effect through suppression of superconductivity. In particular in two spatial dimensions there can be no long-range SDW order at any $T > 0$. These considerations lead us to propose the crossover phase diagram in Fig. 10 in the T, t plane. We anticipate that $t_c(0)$ is near optimal doping. Thus in the underdoped regime above T_c, there is local SDW order that is disrupted by classical thermal fluctuations: this is the so-called "renormalized classical[26]" (RC) regime of the hidden metallic quantum critical point at $t_c(0)$. Going below T_c in the underdoped regime, we eventually reach the regime controlled by the quantum critical point associated with SDW ordering in the superconductor, which is at $t_c(\Delta)$. Because $t_c(\Delta) < t_c(0)$, the SDW order can now be "quantum

disordered" (QD). Thus neutron scattering in the superconductor will not display long-range SDW order as $T \to 0$, even though there is a RC regime of SDW order above T_c. This QD region will have enhanced charge order correlations;[7,16,17,44] this charge order can survive as true long-range order below T_c, even though the SDW order does not. Thus we see that in our theory the underlying competition is between superconductivity and SDW order while there can be substantial charge order in the superconducting phase.

Further study of the nature of the quantum critical point at $t_c(0)$ in the metal is an important direction for further research. In our present formulation in Eq. (1.4), this point is a transition from a conventional metallic SDW state to an "algebraic charge liquid[25]" in the O(4) universality class.[7] However, an interesting alternative possibility is a transition directly to the large Fermi-surface state.[45] Finally, we note that a number of experimental studies[32,46–51] have discussed a scenario for crossover in the cuprates, which is generally consistent with our Fig. 10.

ACKNOWLEDGMENTS

We thank A. Chubukov, V. Galitski, P. D. Johnson, R. Kaul, A. Keren, Yang Qi, L. Taillefer, Cenke Xu, and A. Yazdani for valuable discussions. We are especially grateful to A. Chubukov for pointing out numerical errors in an earlier version of this paper. This research was supported by the NSF under Grant No. DMR-0757145, by the FQXi foundation, and by a MURI grant from USAFOSR. E.G.M. is also supported in part by a Samsung scholarship.

APPENDIX: FIELD RELATIONS FROM SPIN DENSITY WAVE THEORY

This appendix will give a derivation of relation (1.2) between the physical electron operators c_α, and the fields $g_\pm$ and z_α using spin density wave theory. This will complement the derivation obtained from the doped Mott insulator approach in previous works.[7,8]

We begin the quasiparticle Hamiltonian, which determines the "large" Fermi surface in the overdoped regime

$$H_0 = -\sum_{i<j} t_{ij} c_{i\alpha}^\dagger c_{j\alpha} \equiv \sum_{\mathbf{k}} \varepsilon_{\mathbf{k}} c_{\mathbf{k}\alpha}^\dagger c_{\mathbf{k}\alpha}, \tag{A1}$$

where we choose the dispersion $\varepsilon_{\mathbf{k}}$ to agree with the measured Fermi surface. In the presence of spin density wave order $\vec{\varphi}$ at wave vector $\mathbf{K}=(\pi,\pi)$, we have an additional term that mixes electron states with momentum separated by $\mathbf{K}$

$$H_{\rm sdw} = -\vec{\varphi} \cdot \sum_{\mathbf{k},\alpha,\beta} c_{\mathbf{k},\alpha}^\dagger \vec{\sigma}_{\alpha\beta} c_{\mathbf{k}+\mathbf{K},\beta}, \tag{A2}$$

where $\vec{\sigma}$ are the Pauli matrices.

Now we focus on the electrons which are near the electron pockets. Let us write

$$c_{(0,\pi)\alpha} \equiv c_{1\alpha}, \quad c_{(\pi,0)\alpha} \equiv c_{2\alpha}, \tag{A3}$$

and $\varepsilon_{(0,\pi)}=\varepsilon_{(\pi,0)}=\varepsilon_0$. Then, for Néel order polarized as $\vec{\varphi}=(0,0,\varphi)$ with $\varphi>0$, the Hamiltonian for these electrons is

$$H_0 + H_{\rm sdw} = \varepsilon_0 (c_{1\alpha}^\dagger c_{1\alpha} + c_{2\alpha}^\dagger c_{2\alpha}) - \varphi (c_{1\uparrow}^\dagger c_{2\uparrow} - c_{1\downarrow}^\dagger c_{2\downarrow} + c_{2\uparrow}^\dagger c_{1\uparrow} - c_{2\downarrow}^\dagger c_{1\downarrow}). \tag{A4}$$

We diagonalize this by writing

$$H_0 + H_{\rm sdw} = (\varepsilon_0 - \varphi)(g_+^\dagger g_+ + g_-^\dagger g_-) + (\varepsilon_0 + \varphi)(h_+^\dagger h_+ + h_-^\dagger h_-), \tag{A5}$$

where

$$c_{1\uparrow} = (g_+ + h_+)/\sqrt{2},$$
$$c_{2\uparrow} = (g_+ - h_+)/\sqrt{2},$$
$$c_{1\downarrow} = (g_- + h_-)/\sqrt{2},$$
$$c_{2\downarrow} = (-g_- + h_-)/\sqrt{2}. \tag{A6}$$

Now the main approximation we make here is to neglect the higher energy $h_\pm$ fermions. We obtain the electron operators for a general polarization of the Néel order as in Eq. (1.1) by performing an SU(2) rotation defined by the z_α (and dropping the unimportant factor of $1/\sqrt{2}$)

$$\begin{pmatrix} c_{1\uparrow} \\ c_{1\downarrow} \end{pmatrix} = \mathcal{R}_z \begin{pmatrix} g_+ \\ g_- \end{pmatrix}; \quad \begin{pmatrix} c_{2\uparrow} \\ c_{2\downarrow} \end{pmatrix} = \mathcal{R}_z \begin{pmatrix} g_+ \\ -g_- \end{pmatrix}, \tag{A7}$$

where the SU(2) rotation is

$$\mathcal{R}_z = \begin{pmatrix} z_\uparrow & -z_\downarrow^* \\ z_\downarrow & z_\uparrow^* \end{pmatrix}. \tag{A8}$$

These results lead immediately to Eq. (1.2). In the superconducting state, where $\langle g_+ g_- \rangle \neq 0$, they yield

$$\langle c_{1\uparrow} c_{1\downarrow} \rangle = \langle (|z_\uparrow|^2 + |z_\downarrow|^2) g_+ g_- \rangle,$$
$$\langle c_{2\uparrow} c_{2\downarrow} \rangle = -\langle (|z_\uparrow|^2 + |z_\downarrow|^2) g_+ g_- \rangle, \tag{A9}$$

which implies a d-wave pairing signature for the electrons.

[1] N. Doiron-Leyraud, C. Proust, D. LeBoeuf, J. Levallois, J.-B. Bonnemaison, R. Liang, D. A. Bonn, W. N. Hardy, and L. Taillefer, Nature (London) **447**, 565 (2007).

[2] E. A. Yelland, J. Singleton, C. H. Mielke, N. Harrison, F. F. Balakirev, B. Dabrowski, and J. R. Cooper, Phys. Rev. Lett. **100**, 047003 (2008).

[3] A. F. Bangura, J. D. Fletcher, A. Carrington, J. Levallois, M. Nardone, B. Vignolle, P. J. Heard, N. Doiron-Leyraud, D. LeB-

oeuf, L. Taillefer, S. Adachi, C. Proust, and N. E. Hussey, Phys. Rev. Lett. **100**, 047004 (2008).
[4] C. Jaudet, D. Vignolles, A. Audouard, J. Levallois, D. LeBoeuf, N. Doiron-Leyraud, B. Vignolle, M. Nardone, A. Zitouni, Ruixing Liang, D. A. Bonn, W. N. Hardy, L. Taillefer, and C. Proust, Phys. Rev. Lett. **100**, 187005 (2008).
[5] S. E. Sebastian, N. Harrison, E. Palm, T. P. Murphy, C. H. Mielke, Ruixing Liang, D. A. Bonn, W. N. Hardy, and G. G. Lonzarich, Nature (London) **454**, 200 (2008).
[6] D. LeBoeuf, N. Doiron-Leyraud, J. Levallois, R. Daou, J.-B. Bonnemaison, N. E. Hussey, L. Balicas, B. J. Ramshaw, R. Liang, D. A. Bonn, W. N. Hardy, S. Adachi, C. Proust, and L. Taillefer, Nature (London) **450**, 533 (2007).
[7] R. K. Kaul, M. A. Metlitski, S. Sachdev, and C. Xu, Phys. Rev. B **78**, 045110 (2008).
[8] V. Galitski and S. Sachdev, Phys. Rev. B **79**, 134512 (2009).
[9] B. Khaykovich, S. Wakimoto, R. J. Birgeneau, M. A. Kastner, Y. S. Lee, P. Smeibidl, P. Vorderwisch, and K. Yamada, Phys. Rev. B **71**, 220508 (2005).
[10] J. Chang, Ch. Niedermayer, R. Gilardi, N. B. Christensen, H. M. Rønnow, D. F. McMorrow, M. Ay, J. Stahn, O. Sobolev, A. Hiess, S. Pailhes, C. Baines, N. Momono, M. Oda, M. Ido, and J. Mesot, Phys. Rev. B **78**, 104525 (2008).
[11] J. Chang, N. B. Christensen, Ch. Niedermayer, K. Lefmann, H. M. Rønnow, D. F. McMorrow, A. Schneidewind, P. Link, A. Hiess, M. Boehm, R. Mottl, S. Pailhes, N. Momono, M. Oda, M. Ido, and J. Mesot, Phys. Rev. Lett. **102**, 177006 (2009).
[12] D. Haug, V. Hinkov, A. Suchaneck, D. S. Inosov, N. B. Christensen, Ch. Niedermayer, P. Bourges, Y. Sidis, J. T. Park, A. Ivanov, C. T. Lin, J. Mesot, and B. Keimer, Phys. Rev. Lett. **103**, 017001 (2009).
[13] B. Lake, H. M. Rønnow, N. B. Christensen, G. Aeppli, K. Lefmann, D. F. McMorrow, P. Vorderwisch, P. Smeibidl, N. Mangkorntong, T. Sasagawa, M. Nohara, H. Takagi, and T. E. Mason, Nature (London) **415**, 299 (2002).
[14] E. Demler, S. Sachdev, and Y. Zhang, Phys. Rev. Lett. **87**, 067202 (2001); Y. Zhang, E. Demler, and S. Sachdev, Phys. Rev. B **66**, 094501 (2002).
[15] S. A. Kivelson, D.-H. Lee, E. Fradkin, and V. Oganesyan, Phys. Rev. B **66**, 144516 (2002).
[16] S. Sachdev, Rev. Mod. Phys. **75**, 913 (2003).
[17] S. A. Kivelson, I. P. Bindloss, E. Fradkin, V. Oganesyan, J. M. Tranquada, A. Kapitulnik, and C. Howald, Rev. Mod. Phys. **75**, 1201 (2003).
[18] M. Shay, A. Keren, G. Koren, A. Kanigel, O. Shafir, L. Marcipar, G. Nieuwenhuys, E. Morenzoni, M. Dubman, A. Suter, T. Prokscha, and D. Podolsky, arXiv:0906.2047 (unpublished).
[19] Wei-Qiang Chen, Kai-Yu Yang, T. M. Rice, and F. C. Zhang, Europhys. Lett. **82**, 17004 (2008).
[20] S. Sachdev, A. V. Chubukov, and A. Sokol, Phys. Rev. B **51**, 14874 (1995).
[21] A. V. Chubukov and D. K. Morr, Phys. Rep. **288**, 355 (1997).
[22] A. J. Millis and M. R. Norman, Phys. Rev. B **76**, 220503(R) (2007).
[23] N. Harrison, Phys. Rev. Lett. **102**, 206405 (2009).
[24] R. K. Kaul, A. Kolezhuk, M. Levin, S. Sachdev, and T. Senthil, Phys. Rev. B **75**, 235122 (2007).
[25] R. K. Kaul, Y. B. Kim, S. Sachdev, and T. Senthil, Nat. Phys. **4**, 28 (2008).
[26] S. Chakravarty, B. I. Halperin, and D. R. Nelson, Phys. Rev. B **39**, 2344 (1989).
[27] D. J. Scalapino, Phys. Rep. **250**, 329 (1995).
[28] Ar. Abanov, A. V. Chubukov, and J. Schmalian, Adv. Phys. **52**, 119 (2003), and references therein.
[29] K. Park and S. Sachdev, Phys. Rev. B **64**, 184510 (2001).
[30] S. Pathak, V. B. Shenoy, M. Randeria, and N. Trivedi, Phys. Rev. Lett. **102**, 027002 (2009).
[31] H.-B. Yang, J. D. Rameau, P. D. Johnson, T. Valla, A. Tsvelik, and G. D. Gu, Nature (London) **456**, 77 (2008).
[32] W. D. Wise, Kamalesh Chatterjee, M. C. Boyer, Takeshi Kondo, T. Takeuchi, H. Ikuta, Zhijun Xu, Jinsheng Wen, G. D. Gu, Yayu Wang, and E. W. Hudson, Nat. Phys. **5**, 213 (2009).
[33] R. K. Kaul and S. Sachdev, Phys. Rev. B **77**, 155105 (2008).
[34] D. J. Scalapino, *Superconductivity*, edited by R. D. Parks (Marcel Dekker, New York, 1969), Vol. 1.
[35] G. Bergmann and D. Rainer, Z. Phys. **263**, 59 (1973).
[36] A. J. Millis, S. Sachdev, and C. M. Varma, Phys. Rev. B **37**, 4975 (1988).
[37] A. V. Chubukov and J. Schmalian, Phys. Rev. B **72**, 174520 (2005).
[38] We are grateful to Andrey Chubukov for demonstrating this to us.
[39] N. E. Bonesteel, I. A. McDonald, and C. Nayak, Phys. Rev. Lett. **77**, 3009 (1996).
[40] I. Ussishkin and A. Stern, Phys. Rev. Lett. **81**, 3932 (1998).
[41] E. Helfand and N. R. Werthamer, Phys. Rev. **147**, 288 (1966).
[42] M. Schossmann and E. Schachinger, Phys. Rev. B **33**, 6123 (1986).
[43] V. M. Galitski and A. I. Larkin, Phys. Rev. B **63**, 174506 (2001).
[44] M. Vojta and S. Sachdev, Phys. Rev. Lett. **83**, 3916 (1999).
[45] T. Senthil, Phys. Rev. B **78**, 035103 (2008).
[46] M. Vershinin, S. Misra, S. Ono, Y. Abe, Y. Ando, and A. Yazdani, Science **303**, 1995 (2004).
[47] Y. Kohsaka, C. Taylor, P. Wahl, A. Schmidt, Jhinhwan Lee, K. Fujita, J. W. Alldredge, Jinho Lee, K. McElroy, H. Eisaki, S. Uchida, D.-H. Lee, and J. C. Davis, Nature (London) **454**, 1072 (2008).
[48] Y. Kohsaka, C. Taylor, K. Fujita, A. Schmidt, C. Lupien, T. Hanaguri, M. Azuma, M. Takano, H. Eisaki, H. Takagi, S. Uchida, and J. C. Davis, Science **315**, 1380 (2007).
[49] O. Cyr-Choiniere, R. Daou, F. Laliberte, D. LeBoeuf, N. Doiron-Leyraud, J. Chang, J.-Q. Yan, J.-G. Cheng, J.-S. Zhou, J. B. Goodenough, S. Pyon, T. Takayama, H. Takagi, Y. Tanaka, and L. Taillefer, Nature (London) **458**, 743 (2009).
[50] W. D. Wise, M. C. Boyer, Kamalesh Chatterjee, Takeshi Kondo, T. Takeuchi, H. Ikuta, Yayu Wang, and E. W. Hudson, Nat. Phys. **4**, 696 (2008).
[51] T. Helm, M. V. Kartsovnik, M. Bartkowiak, N. Bittner, M. Lambacher, A. Erb, J. Wosnitza, and R. Gross, arXiv:0906.1431 (unpublished).